International Conference on Mathematics and Computational Methods Applied to Nuclear Science and Engineering (M&C 2011)
Rio de Janeiro, RJ, Brazil, May 8-12, 2011, on CD-ROM, Latin American Section (LAS) / American Nuclear Society (ANS)
ISBN 978-85-63688-00-2

AN ANISOTROPIC DIFFUSION APPROXIMATION TO THERMAL RADIATIVE TRANSFER

Seth R. Johnson and Edward W. Larsen
Department of Nuclear Engineering & Radiological Sciences
University of Michigan
2355 Bonisteel Boulevard, Ann Arbor, MI, 48109
sethrj@umich.edu; edlarsen@umich.edu

ABSTRACT

This paper describes an anisotropic diffusion (AD) method that uses transport-calculated AD coefficients to efficiently and accurately solve the thermal radiative transfer (TRT) equations. By assuming weak gradients and angular moments in the radiation intensity, we derive an expression for the radiation energy density that depends on a non-local function of the opacity. This nonlocal function is the solution of a transport equation that can be solved with a single steady-state transport sweep once per time step, and the function's second angular moment is the anisotropic diffusion tensor. To demonstrate the AD method's efficacy, we model radiation flow down a channel in "flatland" geometry.

Key Words: Anisotropic diffusion, Thermal radiative transfer, Flux-limited diffusion, Hybrid methods, Flatland geometry

1. INTRODUCTION

Thermal radiation is the dominant means of energy transfer in a very hot material, such as the interior of a star or the target of a laser-driven shock experiment. The equations describing thermal radiative transfer (TRT) are time-dependent, contain strong nonlinearities, and reside in a large phase space $(\boldsymbol{x}, \boldsymbol{\Omega}, h\nu, t)$. These difficulties make TRT the subject of significant work in methods development, which typically balances fidelity against computational cost. The method described in this paper is meant to be a middle ground between high fidelity transport methods and inexpensive diffusion methods.

Previous work [1] formulated a steady-state anisotropic diffusion (AD) method designed to more accurately model the non-diffusive behavior of voided channels in the Very High Temperature Reactor. This paper extends AD solve the TRT equations for problems containing optically thin channels, as occur in the simulation of certain radiative shocks [2]. By making assumptions about the strength of the gradients and angular moment of the radiative intensity I, we systematically derive an approximate expression for the scalar intensity ϕ. The result is an expression for the radiation flux $\boldsymbol{F}$, a function of the local radiation energy gradient and a nonlocal anisotropic diffusion tensor. The AD tensor is the second angular moment of a steady-state, purely absorbing transport problem with a uniform source.

2. THEORY

We consider the gray TRT equations [3], which eliminate the energy unknown from the full TRT description by approximating the energy dependence of the opacity σ and integrating over all energies. The radiation field is described by a monoenergetic Boltzmann transport equation:

$$\frac{1}{c}\frac{\partial I}{\partial t}(\boldsymbol{x},\boldsymbol{\Omega},t)+\boldsymbol{\Omega}\cdot\boldsymbol{\nabla}I(\boldsymbol{x},\boldsymbol{\Omega},t)+\sigma(\boldsymbol{x},T)I(\boldsymbol{x},\boldsymbol{\Omega},t)=\frac{\sigma(\boldsymbol{x},T)ac[T(\boldsymbol{x},t)]^4}{4\pi}+\frac{cQ(\boldsymbol{x},t)}{4\pi}\,, \tag{1a}$$

and the material energy equation describes the time rate of change in the material energy:

$$\frac{1}{c_v}\frac{\partial T}{\partial t}(\boldsymbol{x},t)=\sigma(\boldsymbol{x},T)\int_{4\pi}I\,\mathrm{d}\Omega-\sigma(\boldsymbol{x},T)ac[T(\boldsymbol{x},t)]^4\,. \tag{1b}$$

Integrating Eq. (1a) over all angles gives an expression for the conservation of energy in the radiation field:

$$\frac{1}{c}\frac{\partial \phi}{\partial t}(\boldsymbol{x},t)+\boldsymbol{\nabla}\cdot\boldsymbol{F}(\boldsymbol{x},t)+\sigma(\boldsymbol{x},T)\phi(\boldsymbol{x},t)=c\sigma(\boldsymbol{x},T)a[T(\boldsymbol{x},t)]^4+cQ(\boldsymbol{x},t)\,. \tag{2}$$

Here the zeroth angular moment of the radiation intensity is the scalar intensity,

$$\phi(\boldsymbol{x},t)\equiv\int_{4\pi}I(\boldsymbol{x},\boldsymbol{\Omega},t)\,\mathrm{d}\Omega\,,$$

which is related to the radiation energy density E by $E=\phi/c$. The first angular moment of I is the radiation flux,

$$\boldsymbol{F}(\boldsymbol{x},t)\equiv\int_{4\pi}\boldsymbol{\Omega}I(\boldsymbol{x},\boldsymbol{\Omega},t)\,\mathrm{d}\Omega\,.$$

If the right hand side of Eq. (1a) is treated as a known time-dependent quantity, the integrodifferential Boltzmann equation can be transformed to an integral transport equation by considering sources and attenuation along the characteristic ray that passes through the point $\boldsymbol{x}$ along $\boldsymbol{\Omega}$ [4]. For simplicity, we consider only the spatiotemporal interior of a problem, where the contribution of the boundary flux and initial condition are exponentially small. With the initial and boundary terms neglected, the integral transport equation is:

$$I(\boldsymbol{x},\boldsymbol{\Omega},t)=\int_0^\infty \mathrm{e}^{-\tau(\boldsymbol{x},\boldsymbol{x}-s\boldsymbol{\Omega},\boldsymbol{\Omega},t)}\hat{Q}(\boldsymbol{x}-s\boldsymbol{\Omega},\boldsymbol{\Omega},t-s/c)\,\mathrm{d}s\,. \tag{3a}$$

The "known" source $\hat{Q}$ is the right hand side in Eq. (1a),

$$\hat{Q}(\boldsymbol{x},\boldsymbol{\Omega},t)=\frac{\sigma(\boldsymbol{x},T[\boldsymbol{x},t])ac[T(\boldsymbol{x},t)]^4}{4\pi}+\frac{cQ(\boldsymbol{x},t)}{4\pi}\,, \tag{3b}$$

which is evaluated along the characteristic ray at a distance s, at the time $t-s/c$ when a particle originating at that point reaches $(\boldsymbol{x},t)$. The optical thickness of the medium between points $\boldsymbol{x}$ and $\boldsymbol{x}'$ along direction $\boldsymbol{\Omega}$ is

$$\tau(\boldsymbol{x},\boldsymbol{x}',\boldsymbol{\Omega},t)=\int_0^{\|\boldsymbol{x}-\boldsymbol{x}'\|}\sigma(\boldsymbol{x}-s'\boldsymbol{\Omega},t-s'/c)\,\mathrm{d}s'\,. \tag{3c}$$

The opacity σ is shown with an implicit dependence on time t because it is a nonlinear function of the temperature $T(\boldsymbol{x}, t)$.

Substituting $\hat{Q}$ into Eq. (3a) gives

$$I(\boldsymbol{x}, \boldsymbol{\Omega}, t) = \frac{1}{4\pi} \int_0^\infty \mathrm{e}^{-\tau(\boldsymbol{x}, \boldsymbol{x}-s\boldsymbol{\Omega}, \boldsymbol{\Omega}, t)} \left[\sigma a c T^4 + cQ\right]_{(\boldsymbol{x}-s\boldsymbol{\Omega}, t-s/c)} \mathrm{d}s \,.$$

The quantity in brackets is just the right-hand side of the conservation equation (2). Replacing it with the left-hand side, we get

$$I(\boldsymbol{x}, \boldsymbol{\Omega}, t) = \frac{1}{4\pi} \int_0^\infty \mathrm{e}^{-\tau(\boldsymbol{x}, \boldsymbol{x}-s\boldsymbol{\Omega}, \boldsymbol{\Omega}, t)} \left[\sigma\phi + \frac{1}{c}\frac{\partial \phi}{\partial t} + \boldsymbol{\nabla} \cdot \boldsymbol{F}\right]_{(\boldsymbol{x}-s\boldsymbol{\Omega}, t-s/c)} \mathrm{d}s \,. \tag{4}$$

We will individually evaluate each constituent term of this integral.

To expand and simplify Eq. (4), it is necessary to make an ansatz about the magnitude of the derivatives and moments of some terms in the transport equation:

$$I = O(1), \quad \sigma = O(1), \quad \boldsymbol{\nabla} I = O(\epsilon), \quad \frac{1}{c}\frac{\partial I}{\partial t} = O(\epsilon), \quad \frac{1}{c}\frac{\partial \sigma}{\partial t} = O(\epsilon), \quad \int_{4\pi} \boldsymbol{\Omega} I \,\mathrm{d}\Omega = O(\epsilon).$$

These assumptions are different (and admittedly less rigorous) than the set traditionally used to derive the radiation diffusion equations [5]. They will lead to an approximate expression for the angular intensity that is *not* linear in angle.

We consider the first term of Eq. (4):

$$\frac{1}{4\pi} \int_0^\infty \mathrm{e}^{-\int_0^s \sigma(\boldsymbol{x}-s'\boldsymbol{\Omega}, t-s'/c)\,\mathrm{d}s'} \sigma(\boldsymbol{x} - s\boldsymbol{\Omega}, t - s/c) \phi(\boldsymbol{x} - s\boldsymbol{\Omega}, t - s/c) \,\mathrm{d}s \,.$$

By the fundamental theorem of calculus, this is equal without approximation to

$$= \frac{1}{4\pi} \int_0^\infty \left(-\frac{\mathrm{d}}{\mathrm{d}s} \mathrm{e}^{-\int_0^s \sigma(\boldsymbol{x}-s'\boldsymbol{\Omega}, t-s'/c)\,\mathrm{d}s'}\right) \phi(\boldsymbol{x} - s\boldsymbol{\Omega}, t - s/c) \,\mathrm{d}s \,.$$

With integration by parts, assuming that ϕ is bounded as $s \to \infty$, this term is

$$\begin{aligned}
&= -\frac{1}{4\pi} \left[\mathrm{e}^{-\int_0^s \sigma(\boldsymbol{x}-s'\boldsymbol{\Omega}, t-s'/c)\,\mathrm{d}s'} \phi(\boldsymbol{x} - s\boldsymbol{\Omega}, t - s/c) \Big|_0^\infty \right. \\
&\qquad \left. - \int_0^\infty \mathrm{e}^{-\int_0^s \sigma(\boldsymbol{x}-s'\boldsymbol{\Omega}, t-s'/c)\,\mathrm{d}s'} \frac{\mathrm{d}}{\mathrm{d}s} \phi(\boldsymbol{x} - s\boldsymbol{\Omega}, t - s/c) \,\mathrm{d}s \right] \\
&= -\frac{1}{4\pi} \left[0 - \mathrm{e}^0 \phi(\boldsymbol{x}, t) - \int_0^\infty \mathrm{e}^{-\tau(\boldsymbol{x}, \boldsymbol{x}-s\boldsymbol{\Omega}, \boldsymbol{\Omega}, t)} \frac{\mathrm{d}}{\mathrm{d}s} \phi(\boldsymbol{x} - s\boldsymbol{\Omega}, t - s/c) \,\mathrm{d}s \right] \\
&= \frac{1}{4\pi} \phi(\boldsymbol{x}, t) + \frac{1}{4\pi} \int_0^\infty \mathrm{e}^{-\tau(\boldsymbol{x}, \boldsymbol{x}-s\boldsymbol{\Omega}, \boldsymbol{\Omega}, t)} \frac{\mathrm{d}}{\mathrm{d}s} \phi(\boldsymbol{x} - s\boldsymbol{\Omega}, t - s/c) \,\mathrm{d}s \,,
\end{aligned}$$

or, rewriting the streaming derivative,

$$= \frac{1}{4\pi} \phi(\boldsymbol{x}, t) + \frac{1}{4\pi} \int_0^\infty \mathrm{e}^{-\tau(\boldsymbol{x}, \boldsymbol{x}-s\boldsymbol{\Omega}, \boldsymbol{\Omega}, t)} \left[-\boldsymbol{\Omega} \cdot \boldsymbol{\nabla} - \frac{1}{c}\frac{\partial}{\partial t}\right] \phi(\boldsymbol{x} - s\boldsymbol{\Omega}, t - s/c) \,\mathrm{d}s \,.$$

So far, no approximations have been made, but the integral involves unknowns at all spatial points along s at prior points in time. Now, using the assumptions about the strength of the derivatives, we approximate the nonlocal unknowns with Taylor series. First, we take a Taylor series in space and time to find $\phi(\boldsymbol{x} - s\boldsymbol{\Omega}, t - s/c)$ about $\phi(\boldsymbol{x}, t)$

$$\begin{aligned}\phi(\boldsymbol{x} - s\boldsymbol{\Omega}, t - s/c) &\sim \phi(\boldsymbol{x}, t) - s\boldsymbol{\Omega}\cdot\boldsymbol{\nabla}\phi(\boldsymbol{x}, t) - s\frac{1}{c}\frac{\partial\phi}{\partial t}(\boldsymbol{x}, t) + \cdots \\ &= \phi(\boldsymbol{x}, t) - s\left[\boldsymbol{\Omega}\cdot\boldsymbol{\nabla} + \frac{1}{c}\frac{\partial}{\partial t}\right]\phi(\boldsymbol{x}, t) + \cdots \\ &= O(1) + O(\epsilon) + \cdots .\end{aligned}$$

Second, we take a Taylor series only in time for the opacity σ embedded in the optical thickness τ:

$$\begin{aligned}\sigma(\boldsymbol{x} - s\boldsymbol{\Omega}, t - s/c) &\sim \sigma(\boldsymbol{x} - s\boldsymbol{\Omega}, t) - s\frac{1}{c}\frac{\partial\sigma}{\partial t}(\boldsymbol{x} - s\boldsymbol{\Omega}, t) + \cdots \\ &= O(1) + O(\epsilon) + \cdots .\end{aligned}$$

The expansion of ϕ allows it to be moved outside the integral, and the expansion of σ obviates the storage of all prior σ:

$$\begin{aligned}&\int_0^\infty \mathrm{e}^{-\int_0^s \sigma(\boldsymbol{x}-s'\boldsymbol{\Omega}, t-s'/c)\,\mathrm{d}s'}\left[-\boldsymbol{\Omega}\cdot\boldsymbol{\nabla} - \frac{1}{c}\frac{\partial}{\partial t}\right]\phi(\boldsymbol{x} - s\boldsymbol{\Omega}, t - s/c)\,\mathrm{d}s \\ &\qquad\sim \int_0^\infty \mathrm{e}^{-\int_0^s \sigma(\boldsymbol{x}-s'\boldsymbol{\Omega}, t)\,\mathrm{d}s'}\,\mathrm{d}s\left[-\boldsymbol{\Omega}\cdot\boldsymbol{\nabla} - \frac{1}{c}\frac{\partial}{\partial t}\right]\phi(\boldsymbol{x}, t) + O(\epsilon^2)\,.\end{aligned}$$

Therefore, the $\sigma\phi$ component of Eq. (4) is approximated as

$$\begin{aligned}&\frac{1}{4\pi}\int_0^\infty \mathrm{e}^{-\tau(\boldsymbol{x}, \boldsymbol{x}-s\boldsymbol{\Omega}, \boldsymbol{\Omega}, t)}\sigma(\boldsymbol{x} - s\boldsymbol{\Omega}, t - s/c)\phi(\boldsymbol{x} - s\boldsymbol{\Omega}, t - s/c)\,\mathrm{d}s \\ &\qquad\sim \frac{1}{4\pi}\underbrace{\phi(\boldsymbol{x}, t)}_{O(1)} + \frac{1}{4\pi}\int_0^\infty \mathrm{e}^{-\int_0^s \sigma(\boldsymbol{x}-s'\boldsymbol{\Omega}, t)\,\mathrm{d}s'}\,\mathrm{d}s\underbrace{\left[-\boldsymbol{\Omega}\cdot\boldsymbol{\nabla} - \frac{1}{c}\frac{\partial}{\partial t}\right]}_{O(\epsilon)}\phi(\boldsymbol{x}, t)\,. \quad (5)\end{aligned}$$

The second component of Eq. (4), the time derivative term, is treated very much like the first: ϕ is expanded about $(\boldsymbol{x}, t)$, and σ is expanded about $(\boldsymbol{x} - s\boldsymbol{\Omega}, t)$. Thus,

$$\begin{aligned}&\frac{1}{4\pi}\int_0^\infty \mathrm{e}^{-\tau(\boldsymbol{x}, \boldsymbol{x}-s\boldsymbol{\Omega}, \boldsymbol{\Omega}, t)}\frac{1}{c}\frac{\partial}{\partial t}\phi(\boldsymbol{x} - s\boldsymbol{\Omega}, t - s/c)\,\mathrm{d}s \\ &\qquad\sim \frac{1}{4\pi}\int_0^\infty \mathrm{e}^{-\int_0^s \sigma(\boldsymbol{x}-s'\boldsymbol{\Omega}, t)\,\mathrm{d}s'}\,\mathrm{d}s\underbrace{\frac{1}{c}\frac{\partial}{\partial t}}_{O(\epsilon)}\phi(\boldsymbol{x}, t)\,. \quad (6)\end{aligned}$$

The time derivative in Eq. (6) exactly cancels the time derivative in Eq. (5) when they are added.

The third ($\boldsymbol{\nabla}\cdot\boldsymbol{F}$) component of Eq. (4), which is the composition of two $O(\epsilon)$ operations, is $O(\epsilon^2)$ and is discarded. Adding the two remaining components together gives the following approximate expression for the angular intensity:

$$I(\boldsymbol{x}, \boldsymbol{\Omega}, t) \approx \frac{1}{4\pi}\phi(\boldsymbol{x}, t) - \left[\int_0^\infty \frac{1}{4\pi}\mathrm{e}^{-\int_0^s \sigma(\boldsymbol{x}-s'\boldsymbol{\Omega}, t)\,\mathrm{d}s'}\,\mathrm{d}s\right]\boldsymbol{\Omega}\cdot\boldsymbol{\nabla}\phi(\boldsymbol{x}, t)\,. \quad (7)$$

Taking the first angular moment of the approximate intensity gives an approximate expression for the radiation flux $\boldsymbol{F}$, which resembles Fick's law:

$$\begin{aligned}
\boldsymbol{F}(\boldsymbol{x},t) &= \int_{4\pi} \boldsymbol{\Omega} I(\boldsymbol{x},\boldsymbol{\Omega},t)\,\mathrm{d}\Omega \\
&= \frac{1}{4\pi}\phi(\boldsymbol{x},t)\int_{4\pi}\boldsymbol{\Omega}\,\mathrm{d}\Omega \\
&\quad - \int_{4\pi}\boldsymbol{\Omega}\left[\int_0^\infty \frac{1}{4\pi}\,\mathrm{e}^{-\int_0^s \sigma(\boldsymbol{x}-s'\boldsymbol{\Omega},t)\,\mathrm{d}s'}\,\mathrm{d}s\right]\boldsymbol{\Omega}\,\mathrm{d}\Omega\cdot\boldsymbol{\nabla}\phi(\boldsymbol{x},t) \\
&\equiv -\left[\int_{4\pi}(\boldsymbol{\Omega}\otimes\boldsymbol{\Omega})f(\boldsymbol{x},\boldsymbol{\Omega},t)\,\mathrm{d}\Omega\right]\cdot\boldsymbol{\nabla}\phi(\boldsymbol{x},t) \\
&\equiv -\mathbf{D}(\boldsymbol{x},t)\cdot\boldsymbol{\nabla}\phi(\boldsymbol{x},t)\,, \qquad (8)
\end{aligned}$$

where $\mathbf{D}$ is the anisotropic diffusion tensor, i.e.,

$$D^{ij}(\boldsymbol{x},t) = \int_{4\pi}\Omega_i\Omega_j f(\boldsymbol{x},\boldsymbol{\Omega},t)\,\mathrm{d}\Omega\,, \qquad (9)$$

and f satisfies the "steady-state" transport equation

$$\boldsymbol{\Omega}\cdot\boldsymbol{\nabla}f(\boldsymbol{x},\boldsymbol{\Omega},t) + \sigma(\boldsymbol{x},t)f(\boldsymbol{x},\boldsymbol{\Omega},t) = \frac{1}{4\pi}\,. \qquad (10)$$

The anisotropic diffusion tensor $\mathbf{D}(\boldsymbol{x},t)$ results from consistent approximations to the transport equation that do not assume that the intensity is linear in angle. However, in an infinite homogeneous (or even optically thick homogeneous) medium, $\mathbf{D} = \mathbf{I}/3\sigma$, which reduces Eq. (8) to Fick's law. Because the solution f is larger along a voided channel than perpendicular to it, the primary action of the tensor $\mathbf{D}$ is along an optically thin channel. More importantly, $\mathbf{D}$ remains bounded in voided regions: it does not "blow up" like a standard diffusion coefficient. Finally, the AD coefficient is spatially continuous, so the solution ϕ will have continuous first derivatives.

The transport problem used to calculate $\mathbf{D}$, Eq. (10), describes a purely absorbing medium with a uniform, isotropic source. It is "steady-state" in the sense that f only depends on the current σ and not on any prior $f(t)$ or other function of t; there is no time-derivative term in that transport equation. Additionally, because the problem has no scattering, and hence no iteratively converging scattering source, *it takes only one transport sweep to solve*. Furthermore, because only the second angular moment needs to be calculated, *solving the transport problem requires no storage of the full angular intensity*: the angular moments can be accumulated as is done in any steady-state transport code. This feature, which provides for a minimal computer memory footprint, helps set the AD method apart from true transport methods such as S_N and quasidiffusion.

The radiation energy conservation equation (2), the material energy conservation equation (1b), the anisotropic diffusion approximation to the radiation flux in Eq. (8), and the transport equation (10) describe the continuous AD equations for TRT. To discretize them in time, we apply the semi-implicit linear approximation [6], which approximates $\sigma(T[t]) \approx \sigma(T^n)$ for $t^n < t < t^{n+1}$. This approximation means that $\mathbf{D}$ is treated explicitly using the old σ^n, and one transport sweep per time step is needed to calculate the AD tensor.

Cell-centered finite differencing is used to spatially discretize the radiation equation. Because the off-diagonal terms of $\mathbf{D}$ imply transverse photon leakage across a cell face, an efficient discretization to account for them is currently unclear. In the implementation used in the numerical test problem, the off-diagonal terms are discarded.[1]

To discretize the transport equation (10), we use the standard S_N formulation with an appropriate quadrature set. Because the method of characteristics [8] can exactly calculate the integral embedded in Eq. (8), it was the obvious (if computationally arduous) method to use. However, numerical experiments suggested that the diamond difference method (with flux fix-up using the step method) yielded $\mathbf{D}$ that were only a few percent different yet saved a factor of five in computational time. The numerical results presented in this paper use diamond difference.

3. NUMERICAL TEST PROBLEM

The benchmark solution is Fleck and Cummings' Implicit Monte Carlo (IMC) method [9], implemented with variance reduction methods and using 10^6 particles per time step. The computationally intensive IMC method correctly prevents photons from exceeding the speed of light, but it is subject to statistical noise and the semi-implicit linearization error.

Also compared is standard diffusion theory, which uses Fick's law to approximate the radiation flux by assuming a linear-in-angle intensity:

$$\boldsymbol{F}_{\mathrm{D}}^{n+1} = -D^n \boldsymbol{\nabla}\phi^{n+1} = -\frac{1}{3\sigma^n}\boldsymbol{\nabla}\phi^{n+1}\,.$$

The time-dependent diffusion equation incorrectly allows radiation energy to propagate faster than c, as does the anisotropic diffusion equation.

The most important competitor for AD is flux-limited diffusion (FLD) [10], which reduces the diffusion coefficient where $\boldsymbol{\nabla}\phi$ is large, preserving the physical limit of $\|\boldsymbol{F}\| < \phi$. As implemented, FLD treats the diffusion coefficient and physics semi-implicitly, and its approximation for the radiation flux is

$$\boldsymbol{F}_{\mathrm{FLD}}^{n+1} = -D^n \boldsymbol{\nabla}\phi^{n+1} = -\left[(3\sigma^n)^2 + \left(\frac{\|\boldsymbol{\nabla}\phi^n\|}{\phi^n}\right)^2\right]^{-1/2} \boldsymbol{\nabla}\phi^{n+1}\,.$$

For the anisotropic diffusion problem, the transport equation that calculates $\mathbf{D}$ uses 16 azimuthal ordinates per quadrant.

3.1 Problem description

One application of the AD method is in the Center for Radiative Shock Hydrodynamics [2], which requires numerous radiation transport simulations to perform uncertainty quantification.

[1] We derived and implemented a discretization, similar to Gol'din's method [7], that stores ϕ at both cell centers and cell edges. The addition of these extra unknowns reduces the computational efficiency and, from limited testing, appears to change the solution only slightly.

A mock-up of their primary problem of interest, a radiation shock traveling down a tube filled with xenon, serves as the primary test case in this work.

The problem models radiation flowing down a pipe in flatland geometry, where photons are constrained to the plane. (This contrasts 2D geometry, where a gap extends infinitely into and out of the page.) It uses scaled units with $c = a = 1$. Fig. 1 shows the material layout for the problem. The source has a volumetric source $Q = 1$ for $0 \leq t \leq 1$ and turns off at $t = 1$;

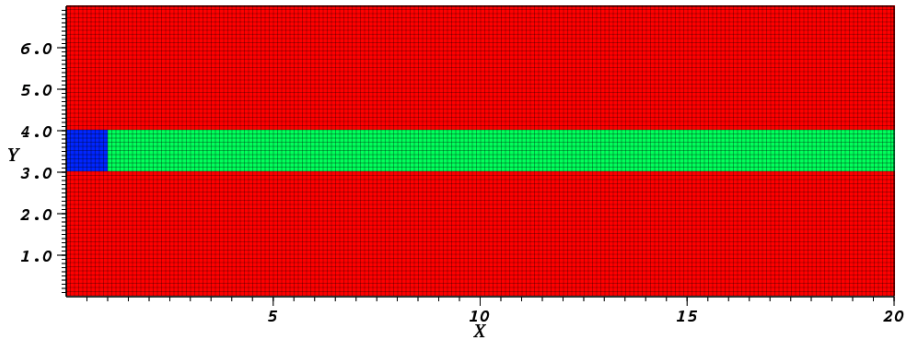

Figure 1: Material properties for the pipe problem. The blue square is the source, the green channel is a low-opacity region, and the red regions are diffusive.

it has a heat capacity $c_v = 0.5$ and opacity $\sigma = 0.5$. The diffusive region has a small heat capacity $c_v = 0.1$, and an inverse cubic opacity, $\sigma = T^{-3}$. The streaming channel region has $c_v = 0.1$ and $\sigma = 0.01T^{-3}$. The material temperature and radiation temperature ($acT_{\text{rad}}^4 = \phi$) are $T = T_{\text{rad}} = 0.1$. The left boundary is reflecting, and the others are vacuum.

The spatial grid is uniform with $\Delta_x = 0.1$. The time grid is linearly increasing and then constant: $\Delta_t(t) \approx 0.1t + 0.099(1 - t)$ for $0 \leq t < 1$, then $\Delta_t = 0.1$ for $1 \leq t < 10$. A more resolved time step at the beginning is a common technique to reduce the effect of the linearization error (i.e., to prevent a violation of the maximum principle) and to improve the behavior of the explicitly treated FLD coefficient.

3.2 Results

Figure 2 shows the material temperature T as calculated by the four methods at increasing times. Figure 3 shows the scalar intensity ϕ for the four methods. The injected radiation energy heats up the material, reducing the opacity of both the diffusive and channel regions. As the material grows more optically thin, energy is more easily transferred there from the source, causing a wavefront in the radiation and material temperatures.

Because the channel is so thin, the radiation travels through it relatively unhindered. Of the compared methods, only IMC correctly simulates the finite speed of particles. FLD does a good job of approximating the finite energy propagation speed by modifying the diffusion coefficients at the wavefronts, where there is a strong spatial gradient. Both AD and standard diffusion allow energy to move faster than c, but because AD yields comparatively smaller diffusion coefficients, the radiation flux is smaller.

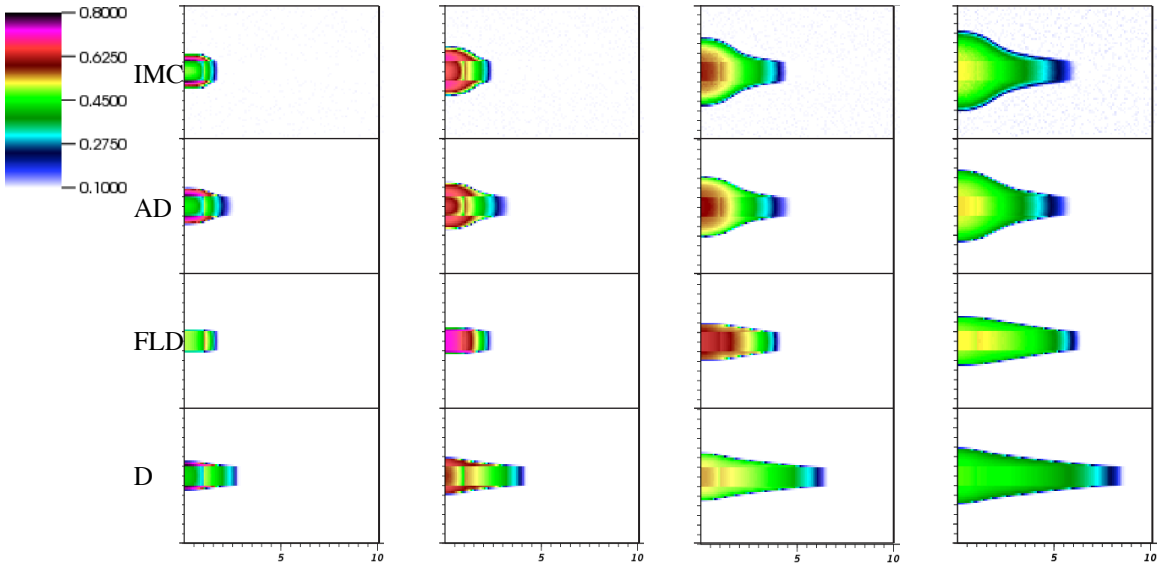

Figure 2: Pseudocolor plot of material temperature for the four methods (top to bottom: IMC, AD, FLD, diffusion) at $t = 1$, 2, 5, and 10.

Both standard and flux-limited diffusion also have notable errors in their modeling of the diffusive region. With standard diffusion, because the same amount of energy is distributed throughout a much larger region of the channel, the average temperature is colder, so the penetration rate into the surrounding diffusive medium is incorrectly small. Flux limiting has the side effect of modifying the diffusion coefficient in diffusive regions because of the steep radiation energy gradient. This unphysically limits the spread of radiation into the walls, bottling energy in the channel.

The diffusion coefficients, as plotted at the final time in Fig. 4, offer an insightful comparison between the three diffusion methods. In the optically thin channel, anisotropic diffusion produces coefficients an order of magnitude smaller than standard diffusion. Because of the tendency for photons to stream down the channel rather than across it, $D^{xx} > D^{yy}$. In this problem, the magnitude of the D^{xy} terms (which can be negative, positive, or zero) is very small compared to the other components D^{xx} and D^{yy}, justifying the approximation of neglecting them.

Figure 5 plots the anisotropic diffusion tensors as ellipses, where the axes of an ellipse are oriented along the eigenvectors of $\mathbf{D}$ at that point, scaled proportionally to the eigenvalues. Isotropic $\mathbf{D}$ appear as circles sized proportionally to $\|\mathbf{D}\|$, and anisotropic tensors point along the direction that particles preferentially flow. In the optically thin channel, the anisotropic diffusion coefficients are larger and directed along the channel. In the thicker parts of the problem, they are isotropic. The apparent asymmetry about the channel centerline is an artifact of the visualization.

Comparing relative wall times for the methods shows that the additional accuracy of AD comes at only a small computational cost. Flux-limited diffusion and standard diffusion ran equally fast, anisotropic diffusion took about 60% longer than FLD, and the benchmark IMC solution took about 40 times longer than the AD calculation. Doubling the number of ordinates used to calculate $\mathbf{D}$ increased the run time by 70% with only a few percent change in the answer.

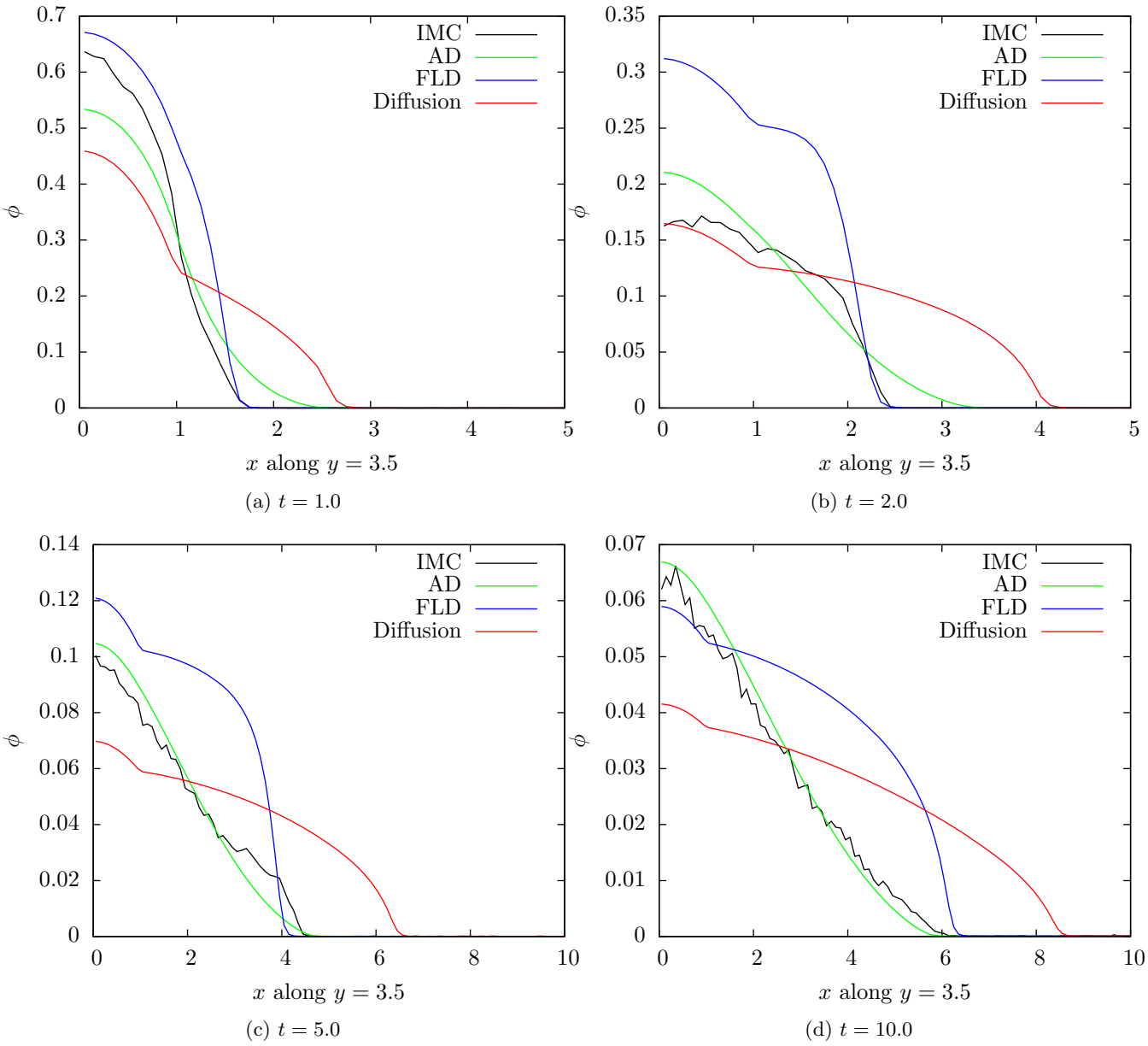

(a) $t = 1.0$ (b) $t = 2.0$

(c) $t = 5.0$ (d) $t = 10.0$

Figure 3: Scalar intensity along the center of the channel at $t = 1, 2, 5, 10$

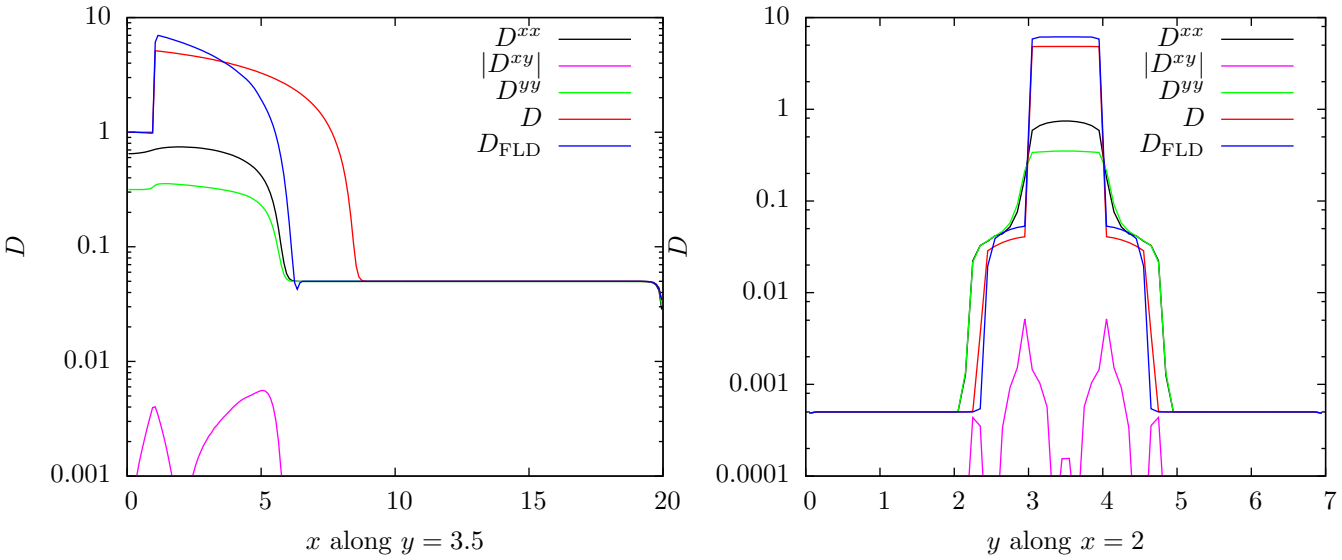

(a) Along the channel centerline

(b) Perpendicular to the channel

Figure 4: Diffusion coefficients at $t = 10$.

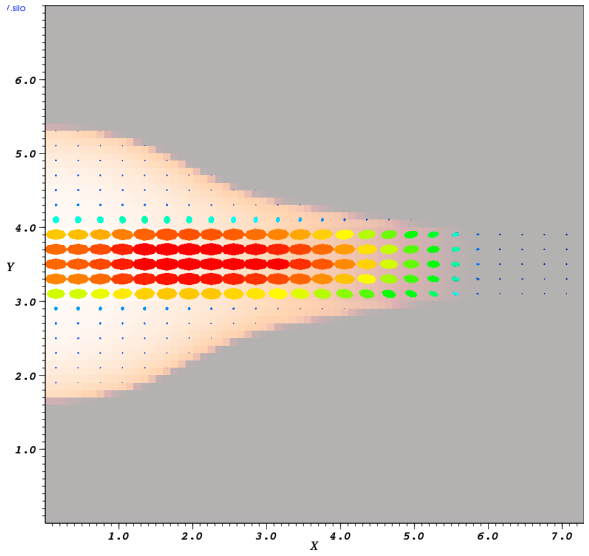

Figure 5: Anisotropic diffusion tensors at $t = 10$ overlaid on the material temperature.

4. CONCLUSIONS

The anisotropic diffusion method accounts for some amount of arbitrary anisotropy in the angular intensity, unlike standard or flux-limited diffusion, by preserving some transport physics. It works best in problems with weaker derivatives, as suggested by theory and borne out by numerical experiments.

The currently implemented AD method has several deficiencies whose resolution could make the method even more accurate. First, we desire to improve the behavior at the leading edge of the wavefront by limiting the energy propagation speed to c. Additionally, a more careful study of the boundary and initial conditions should be undertaken. Finally, we should quantify the penalty of omitting the D^{xy} terms for various problems, or find an effective discretization scheme that accounts for that transverse leakage.

The AD method could also be made more computationally efficient by reducing the time spent in transport sweeps, possibly by evaluating $\mathbf{D}$ on coarser spatial grid, since it is smooth; updating $\mathbf{D}$ less frequently than every time step; or using an advanced quadrature set for *a priori* problem geometries.

Overall, the AD method shows promise for being a computationally efficient but accurate method for approximately solving the TRT equations.

ACKNOWLEDGEMENTS

This material is based upon work supported under a National Science Foundation Graduate Research Fellowship and a Department of Energy Nuclear Energy University Programs Graduate Fellowship.

REFERENCES

1. E. W. Larsen and T. J. Trahan, 2-D Anisotropic Diffusion in Optically Thin Channels, in Trans. Am. Nucl. Soc., (2009), vol. 101, pp. 387–389.

2. R. P. Drake, M. L. Adams, K. G. Powell, and Q. F. Stout, Center for Radiative Shock Hydrodynamics Project Year 2 Report, http://aoss-research.engin.umich.edu/crash/ (2010).

3. G. C. Pomraning, *The Equations of Radiation Hydrodynamics*, Dover Publications, Inc., Mineola, New York (1973).

4. A. K. Prinja and E. W. Larsen, *Handbook of Nuclear Engineering: General Principles of Neutron Transport*, Springer (2010).

5. E. W. Larsen, G. C. Pomraning, and V. C. Badham, Asymptotic Analysis of Radiative Transfer Problems, *Journal of Quantitative Spectroscopy and Radiative Transfer*, **29**, 4, pp. 285–310 (1983).

6. E. W. Larsen, A Grey Transport Acceleration Method for Time-Dependent Radiative Transfer Problems, *Journal of Computational Physics*, **78**, 2, pp. 459–480 (1988).

7. W. A. Wieselquist, *The Quasidiffusion Method for Transport Problems on Unstructured Meshes*, Ph.D. thesis, North Carolina State University (2009).

8. J. R. Askew and M. J. Roth, WIMS-E: A Scheme for Neutronics Calculations, Tech. Rep. AEEW-R-1315, United Kingdom Atomic Energy Authority (1982).

9. J. A. Fleck, Jr. and J. D. Cummings, An Implicit Monte Carlo Scheme for Calculating Time and Frequency Dependent Nonlinear Radiation Transport, *Journal of Computational Physics*, **8**, 3, pp. 313–342 (1971).

10. G. L. Olson, L. H. Auer, and M. L. Hall, Diffusion, P_1, and other approximate forms of radiation transport, *Journal of Quantitative Spectroscopy and Radiative Transfer*, **64**, pp. 619–634 (2000).